Review Article

Imaging of non alcoholic fatty liver disease: A road less travelled

Divya Singh, Chandan J. Das, Manas P. Baruah[1]

Department of Radiology, All India Institute of Medical Sciences, New Delhi, [1]Department of Endocrinology, Excel Center, Guwahati, Assam, India

ABSTRACT

Non alcoholic fatty liver disease (NAFLD) is a spectrum that includes simple steatosis, nonalcoholic steatohepatitis and cirrhosis. It is increasingly emerging as a cause of elevated liver enzymes, cryptogenic cirrhosis and hepatocellular carcinoma. The morbidity and mortality related to NAFLD is expected to rise with the upsurge of obesity and type 2 diabetes mellitus. The need of the hour is to devise techniques to estimate and then accurately follow-up hepatic fat content in patients with NAFLD. There are lots of imaging modalities in the radiological armamentarium, namely, ultrasonography with the extra edge of elastography, computed tomography, and magnetic resonance imaging with chemical shift imaging and spectroscopy to provide an estimation of hepatic fat content.

Key words: Chemical shift imaging, computed tomography, hepatic steatosis, MR spectroscopy, non alcoholic fatty liver disease, sonoelastography

Introduction

Non alcoholic fatty liver disease (NAFLD) has today been recognized as the most common cause of abnormal liver function among adults in the United States.[1] It is a cause of liver disease to reckon with in the Indian population. Various epidemiological studies have placed the prevalence of NAFLD from 9% to 32% of general population in India.[2] NAFLD is a spectrum that includes simple steatosis and nonalcoholic steatohepatitis (NASH). It is increasingly emerging as a cause of elevated liver enzymes, cryptogenic cirrhosis, and hepatocellular carcinoma. In recent times, the prevalence of NAFLD has been increasing in the pediatric population, thereby increasing its overall impact.[3] Efforts are underway to develop novel therapies to combat this global problem. Liver biopsy has been the gold standard for determination of hepatic steatosis and accompanying changes. However, this procedure is invasive with several drawbacks. These limitations have prompted investigators to devise non-invasive, "painless", reliable alternatives to detect and quantify liver fat. There are a host of imaging modalities in the radiological armamentarium, namely, ultrasonography (USG) with the extra edge of elastography, computed tomography (CT), and magnetic resonance imaging (MRI) with chemical shift imaging (CSI) and spectroscopy to provide an estimation of hepatic fat content.

Access this article online	
Quick Response Code:	Website: www.ijem.in
	DOI: 10.4103/2230-8210.122606

Pathophysiology

Various mechanisms have been put forth to explain the pathogenesis of NASH. The "multiple hit" hypothesis is the most widely accepted. This proposes first "hit" as the development of hepatic macrosteatosis as a result of increased lipolysis and free fatty acid levels. The increase in the reduction of free fatty acid oxidation with insulin resistance leads to fatty acid accumulation. Several possible "second hits" may be oxidative stress from reactive oxygen species in the mitochondria and cytochrome P450 enzymes, endotoxins, cytokines, adipokines and environmental factors [Figure 1]. Central obesity with visceral fat and

Corresponding Author: Dr. Chandan J Das, Department of Radiology, All India Institute of Medical Sciences, New Delhi - 29, India.
E-mail: docchandan17@gmail.com

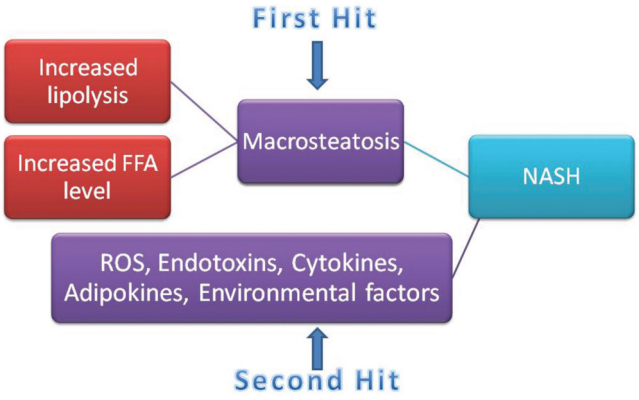

Figure 1: Pathophysiology of non alcoholic fatty liver disease

white adipose deposition is a major source of adipokines and cytokines. Adipokines released from white adipose tissue include adiponectin (protective), leptin (pro-fibrotic), and resistin (mediator of insulin resistance). The proinflammatory cytokines released from white adipose tissue include tumor necrosis factor alpha (TNF-α) and interleukin-6.[4]

Imaging Modalities

Ultrasonography

USG is a safe, radiation-free, easily available, cost-effective way of determining fatty infiltration of liver. The examination can be performed using a 2-5 MHz convex transducer. The normal liver parenchyma has a homogeneous echotexture with echogenicity equal to or slightly greater than that of the renal cortex and spleen. The liver shows echogenicity higher than the renal cortex and spleen due to fatty infiltration.[5] Various (0-3) grades of steatosis have been proposed based on visual analysis of the intensity of the echogenicity, provided that the gain setting is optimum [Figure 2]. When the echogenicity is just increased, it is grade I; when the echogenic liver obscures the echogenic walls of portal vein branches, it is grade II, and, when the echogenic liver obscures the diaphragmatic outline, it is grade III fatty infiltration.[6] These are however subject to inter-observer variation. The sensitivity of USG in detecting hepatic steatosis ranges from 60 to 94% and the specificity from 84 to 95%.[7-9] Hepatorenal sonographic index, which is the ratio between the mean brightness level of the liver and the right kidney, has also been proposed as a measure of hepatic steatosis with a cut-off of 1.49, yielding very high sensitivity (100%) and specificity (91%) for the diagnosis of steatosis >5%.[10] Transient elastography/Fibroscan and acoustic radiation force impulse (ARFI) elastography can be integrated into the conventional USG system. These have emerged as new kids on the block to grade the extent of liver stiffness.

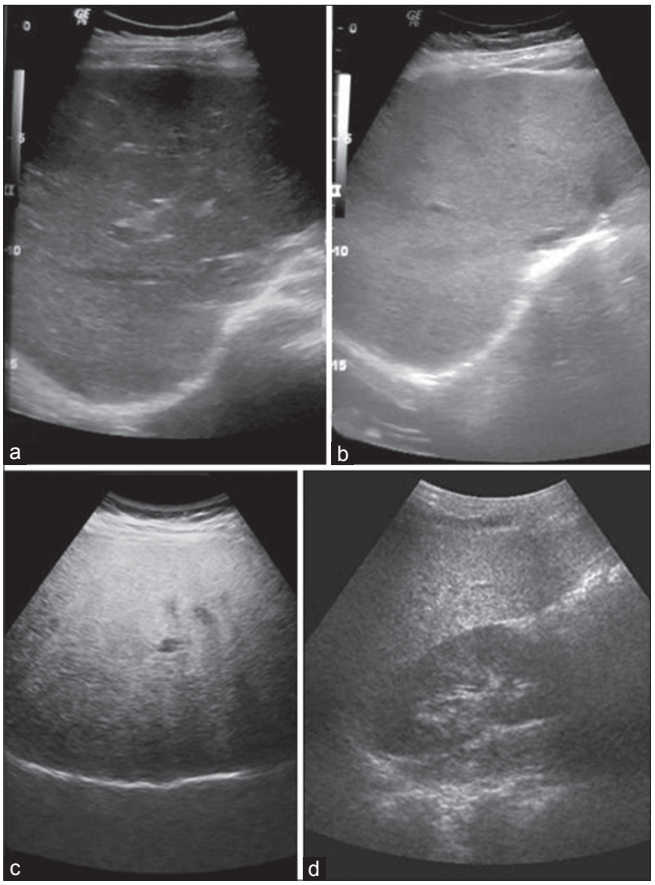

Figure 2: Grades of fatty liver on visual analysis. Ultrasound image shows (a) Normal liver echogenicity (b) Grade 1 fatty liver with increased liver echogenicity (c) Grade 2 fatty liver with the echogenic liver obscuring the echogenic walls of the portal venous branches (d) Grade 3 fatty liver in which the diaphragmatic outline is obscured

Sonoelastography

Principle

Sonoelastography provides an estimation of liver stiffness that in turn is affected by fat infiltration and includes techniques such as ARFI and transient elastography. ARFI imaging involves targeting an anatomic region to be examined for its elastic properties by using a region-of-interest cursor while performing real-time B-mode imaging. The measured shear wave speed is an intrinsic and reproducible property of tissue. By observing the shear wave front at several locations and correlating these measurements with the elapsed time, the shear wave speed can be quantified. Tracking beams, which are sensitive to greater than 1/100 the wavelength of sound, are applied adjacent to the push pulse path. These beams are continuously transmitted until the passing shear wave front is detected. The time between the generation of the shear wave and the detection of the peak is used to compute the shear wave velocity. In transient elastography, a pulse-echo acquisition is performed to follow the propagation of the shear wave and measure its velocity, which is directly related to the tissue stiffness (or elastic modulus). The results are

expressed in kilopascals (kPa). The harder the tissue, the faster the propagation of the shear wave.[11,12]

Technique

Transient elastography/Fibroscan measures liver stiffness as a function of the extent of hepatic infiltration. It is performed with a curved array US probe at 4 MHz for B-mode imaging. The patient is positioned supine on the couch with the right arm in maximum abduction, which makes the right hypochondrium accessible. Normal breathing is recommended. The tip of the transducer is covered with 5 mm of USG gel and placed on the skin in the selected intercostal space with a pressure of the probe such that it is absorbed by the ribs without impacting the soft tissue. B-mode image is obtained by avoiding the rib shadowing and focusing on the right lobe of the liver. After ensuring the best possible contact between the probe and the skin, a switch to elastography mode is made and shear wave elastography (SWE) box is obtained. The box is moved onto a vessel-free region of liver parenchyma, which is defined by the B-mode image. An area where the liver tissue is at least 6-cm thick and free of large blood vessels is selected. A measurement depth of 2 cm below the liver capsule may be chosen to standardize the examination. The quantification is then performed by choosing a size ranging from 15 to 20 mm, preferably in the central area of the SWE box having an area of relative homogeneous elasticity displayed in different colors [Figure 3]. The shear stiffness of normal liver is between 6.5 and 7 kPa. Several (as many as ten) successful acquisitions should be performed in each patient, and the median value should be determined and used as a representative measurement of the liver elasticity.

ARFI is also performed in a similar fashion, and it measures shearing velocity. Normal velocity of liver is 1 m/s. This velocity decreases once there is fatty infiltration [Figure 4].

Computed tomography

Steatosis causes reduced attenuation of liver on CT, which can be represented quantitatively by comparing it with the attenuation of spleen on unenhanced scans. A liver-to-spleen attenuation ratio of <0.8 has a high specificity (100%) for diagnosis of moderate to severe steatosis. From the assessment of hepatic steatosis in transplant donors, it has been concluded that unenhanced CT performs very well in diagnosing steatosis of ≥ 30%, with 100% specificity and 82% sensitivity.[13] Calculating the difference between the attenuation of the spleen and that of the liver can also be used to evaluate steatosis. The attenuation of the spleen is approximately 8-10 HU less than that of the liver in a normal individual, whereas a liver-to-spleen attenuation difference >10 HU is a strong predictor of hepatic steatosis.[14] It is a quick, non-operator dependent technique. Radiation exposure can be kept at a minimum by using low-dose protocols.

Dual-energy CT can also be used to quantify hepatic fat. It involves acquisition at two tube potentials, namely, 80 and 140 kVp. The estimation of tissue composition is possible due to the difference in the attenuation characteristics of different substances. In hepatic steatosis, there is a decrease in CT attenuation of liver at low energy level. As the tube potential increases, the fat attenuation increases. Studies have found that an attenuation change of >10 HU with increase in tube potential from 80 to 140 kVp is suggestive of fatty infiltration of >25%.[15]

Principle

The degree of decrease in attenuation on unenhanced CT is the best predictor of the degree of fatty infiltration in the liver.[16]

Technique

Low-dose, unenhanced CT (80 kV, 100 mAs with dose modulation, collimation of 128 × 0.625, 10-mm section thickness) is performed. For each case, the hepatic attenuation [Figure 5] is measured by means of a random selection of circular regions of interest (ROIs) on both lobes. For each ROI, the largest possible ROI is selected

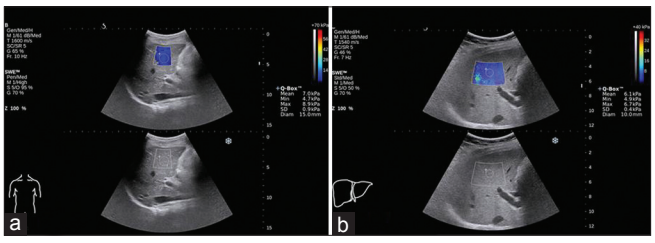

Figure 3: Shear wave elastography. Sonoelastography image (a) shows normal liver with mean stiffness value of 7.0 kilopascal (b) grade 1 fatty liver showing decrease in the mean stiffness value to 6.1 kilopascal

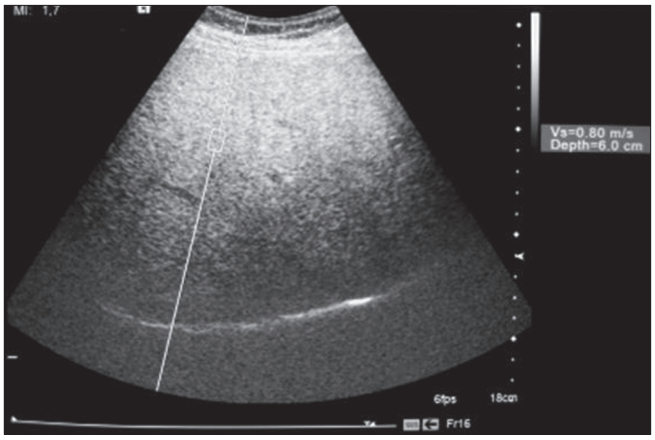

Figure 4: Acoustic radiation force impulse (ARFI) elastography. Sonoelastography image shows grade 2 fatty liver with decrease in shearing velocity (0.80 m/sec). The shearing velocity in normal liver parenchyma is 1 m/s

by avoiding areas of visible hepatic vascular and biliary structures. ROIs may range from 200 to 400 mm^2. The ROI values are averaged as a mean hepatic attenuation. To provide an internal control, the mean splenic attenuation is also calculated by averaging three random ROI values of splenic attenuation measurement. The largest possible ROI (size range: 200-400 mm^2) is selected to represent splenic parenchymal attenuation. The liver attenuation index (LAI) is derived from the difference between mean hepatic attenuation and mean splenic attenuation and can be used as a parameter for prediction of the degree of macrovesicular steatosis. A difference in attenuation of the liver and spleen of 10 HU is taken as normal.

Magnetic resonance imaging

MRI is a radiation-free modality to detect hepatic fat even in microscopic quantity. Various techniques like CSI, proton spectroscopy, and MR elastography can be utilized. The sensitivity and specificity of CSI is 90% and 91%, while that of spectroscopy is 91% and 87%, respectively.[17] MR elastography can be used to measure liver stiffness. However, MRI is a relatively time consuming and costly procedure.

Principle

CSI is based on the fact that during echo time (TE), the transverse magnetization vectors of fat and water develop a phase difference that results in decreased overall length of the magnetization vector under opposed phase (OP) conditions. At the main magnetic field strength of 1.5 T, the frequency shift between fat and water is approximately 220 Hz, which results in OP condition at a TE of about 2.4 ms and in-phase (IP) condition at a TE of about 4.8 ms. Typically, the fatty liver shows increase in signal intensity (SI) on IP images and shows diffuse signal drop in OP image. The fat fraction can then be determined by calculating the loss of SI in OP images as compared to IP images [Figure 6]. From congruent sets of IP and OP images, acquired within the same breath-hold, the fat fraction can be calculated pixel-wise, and misregistration errors can be avoided. Thus, maps of intrahepatic fat fraction and fat signal percentage can be obtained to estimate liver fat content and show differences in regional fat distribution. A commonly used formula for calculating the hepatic fat signal percentage (FSP) is $[(SI_{IP} - SI_{OP})/2SI_{IP}] \times 100$. Where, SI_{IP} is the ratio of hepatic to splenic SI in the IP image and SI_{OP} is the ratio of hepatic to splenic SI in the T1-weighted OP image. Breath-hold gradient-echo (GRE) is the chemical shift technique routinely used for fat estimation. However, GRE sequences are susceptible to the paramagnetic effects of iron. Hence, Dixon put forth the two-point method for CSI using spin echo (SE) sequence. The IP images were the unmodified SE images, whereas the OP images were generated by offsetting the rephasing pulse in a SE sequence. Summation and subtraction yielded the water-only and fat-only images, which could be used for direct quantification.[18-20] The limitation of this technique was its long acquisition time and sensitivity to magnetic field inhomogeneities. To overcome these, a three-point Dixon method was introduced, which involved acquisition of a third set of images besides the in- and opposed-phase images.

Modified GRE techniques have been developed to decrease acquisition time and to eliminate misregistration and susceptibility to magnetic field inhomogeneities. With these techniques, the IP and OP images are acquired within a matter of milliseconds by using different TEs in the same acquisition. The advantages of CSI are coverage of the entire liver.

Two main strategies are used for single-voxel spectroscopy (SVS), namely, point-resolved spectroscopy (PRESS) or

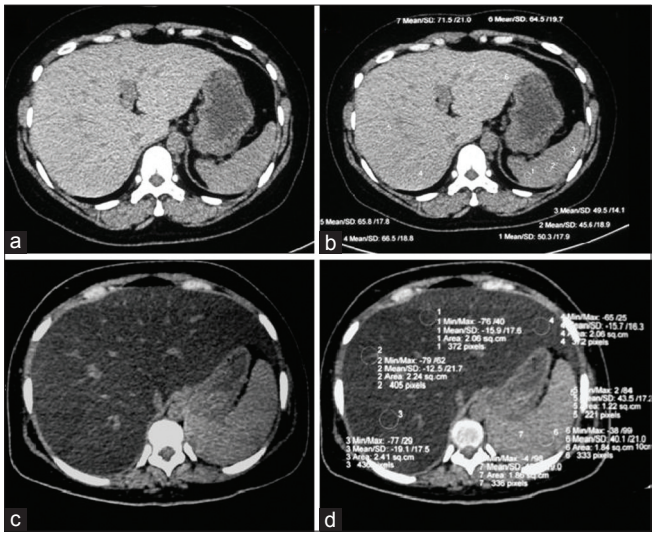

Figure 5: CT for detection of liver fat. Image shows (a) normal liver with attenuation greater than spleen on visual analysis (b) multiple ROIs for measurement of attenuation of liver and spleen, mean hepatic attenuation is 67 HU and mean splenic attenuation is 48.5 HU, hence, liver attenuation index LAI is 18.5 HU which is normal (c) diffuse fatty infiltration of liver with hepatic attenuation markedly less than the spleen (d) multiple ROIs show mean hepatic attenuation of –15.8 HU and mean splenic attenuation of 42.5 HU with LAI of -58.3 HU suggestive of marked fatty infiltration of liver

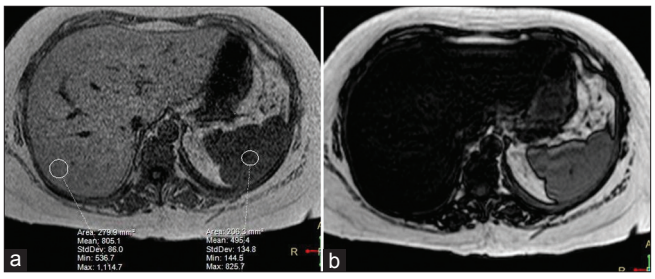

Figure 6: Chemical shift imaging. MRI image shows (a) in-phase image with a hepatic to splenic signal intensity ratio of 1.6 (b) opposed- phase shows signal drop in liver due to diffuse fatty infiltration

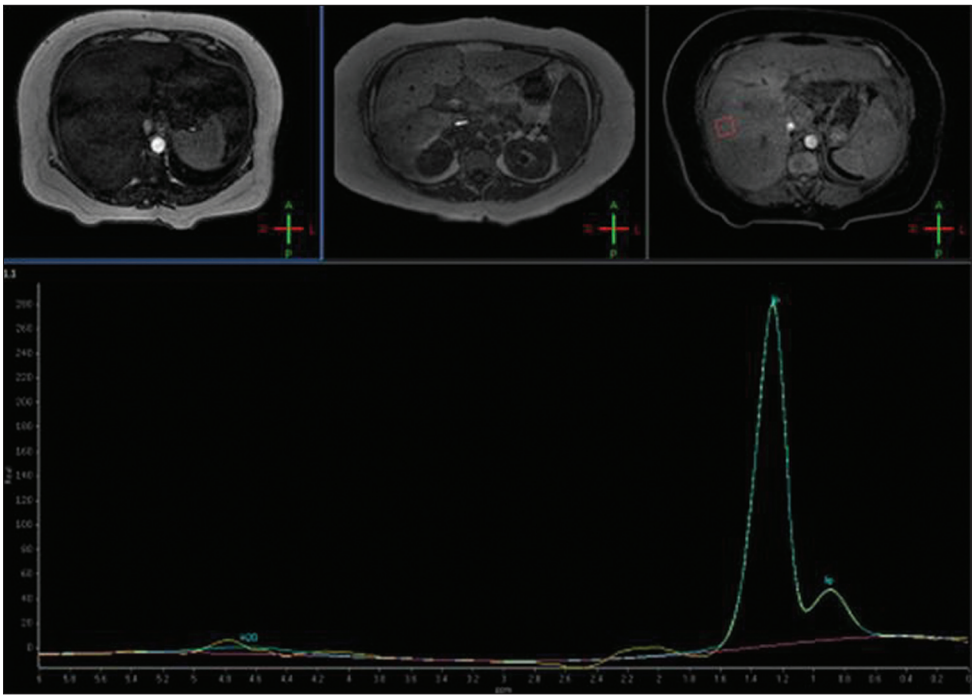

Figure 7: MR Spectroscopy PRESS. Image shows a lipid peak (white arrow) in a case of hepatic steatosis

stimulated-echo acquisition mode (STEAM).[21] The PRESS acquisition scheme (multi-echo single-shot technique) uses a 90°-180°-180° pulse sequence with long TE and allows better visualization of metabolites with long T1 relaxation times. In contrast, the STEAM sequence applies a 90°-90°-90° pulse sequence and is less sensitive to J-coupling effects. The STEAM sequence provides shorter TE and lower signal yield as compared to PRESS, which is usually not a limitation for fat quantification in the liver.

Technique

MRI with CSI involves acquisition of T1-weighted IP and OP images. The SI is measured by mean ROI placed at same locations in both phases. Several (as many as 12) ROIs may be placed in the liver at three levels, with four ROIs at each level (two in the right lobe and two in the left lobe) on anatomically matched locations on the IP and out-of-phase T1-weighted MRI. All of the ROIs should have an area between 1.5 and 2 cm^2 (volume, 1.2-1.6 cm^3) and should avoid major vessels, organ edges, or visual artifacts. The ROIs can be placed superior, inferior, and at the level of the portal vein. This generates a maximum of 12 ROIs in the liver on both the IP and out-of-phase images, which are averaged together to create the average SI value of the IP image and out-of-phase image. Fat-water ratio can be obtained by dividing SI of liver in OP sequence by SI of liver in IP sequence.

MR spectroscopy (MRS) shows an increase in the intensity of the lipid resonance peak in the presence of steatosis at 1.9-2.3 parts per million (ppm), 1.1-1.5 ppm, and 0.8-1.1 ppm [Figure 7]. Because MRS allows the direct measurement of the area under the lipid resonance peak, it can be used to provide a quantitative assessment of fatty infiltration of the liver. It is also unaffected by confounding factors like fibrosis, iron overload, and glycogen. However, it is a complex technique that requires patient co-operation and samples only a small portion of the entire liver.

To conclude, NAFLD is significant cause of chronic liver disease and is now regarded as hepatic manifestation of the metabolic syndrome. The morbidity and mortality related to NAFLD is expected to rise with the upsurge of obesity and type 2 diabetes mellitus. The need of the hour is to devise techniques to estimate and then accurately follow-up hepatic fat content in patients with NAFLD. Since efforts are underway to treat this condition, it is of paramount importance to come up with accurate, reproducible, and non-invasive means of estimating liver fat. Imaging modalities like sonoelastography, CT, and MRI are the front runners in quantification of hepatic steatosis in this manner and may do away with the need of an invasive liver biopsy for this indication in the near future.

References

1. Clark JM, Brancati FL, Diehl AM. The prevalence and etiology of elevated aminotransferase levels in the United States. Am J Gastroenterol 2003;98:960-7.
2. Duseja A. Nonalcoholic fatty liver disease in India: A lot done, yet more required! Indian J Gastroenterol 2010;29:217-25.
3. Manco M, Bottazzo G, DeVito R, Marcellini M, Mingrone G,

Nobili V. Nonalcoholic fatty liver disease in children. J Am Coll Nutr 2008;27:667-76.
4. Edmison J, McCullough AJ. Pathogenesis of non-alchoholic steatohepatitis: Human data. Clin Liver Dis 2007;11:75-104.
5. Valls C, Iannacconne R, Alba E, Murakami T, Hori M, Passariello R, *et al*. Fat in the liver: Diagnosis and characterization. Eur Radiol 2006;16:2292-308.
6. Saadeh S, Younossi ZM, Remer EM, Gramlich T, Ong JP, Hurley M, *et al*. The utility of radiological imaging in nonalcoholic fatty liver disease. Gastroenterology 2002;123:745-50.
7. Joseph AE, Saverymuttu SH, al-Sam S, Cook MG, Maxwell JD. Comparison of liver histology with ultrasonography in assessing diffuse parenchymal liver disease. Clin Radiol 1991;43:26-31.
8. Debongnie JC, Pauls C, Fievez M, Wibin E. Prospective evaluation of the diagnostic accuracy of liver ultrasonography. Gut 1981;22:130-5.
9. Saverymuttu SH, Joseph AE, Maxwell JD. Ultrasound scanning in the detection of hepatic fibrosis and steatosis. Br Med J (Clin Res Ed) 1986;292:13-5.
10. Webb M, Yeshua H, Zelber-Sagi S, Santo E, Brazowski E, Halpern Z, *et al*. Diagnostic value of a computerized hepatorenal index for sonographic quantification of liver steatosis. AJR Am J Roentgenol 2009;192:909-14.
11. Yoneda M, Suzuki K, Kato S, Fujita K, Nozaki Y, Hosono K, *et al*. Nonalcoholic fatty liver disease: US-based acoustic radiation force impulse elastography. Radiology 2010;256:640-7.
12. Sandrin L, Fourquet B, Hasquenoph JM, Yon S, Fournier C, Mal F, *et al*. Transient elastography: A new noninvasive method for assessment of hepatic fibrosis. Ultrasound Med Biol 2003;29:1705-13.
13. Park SH, Kim PN, Kim KW, Lee SW, Yoon SE, Park SW, *et al*. Macrovesicular hepatic steatosis in living liver donors: Use of CT for quantitative and qualitative assessment. Radiology 2006;239:105-12.
14. Piekarski J, Goldberg HI, Royal SA, Axel L, Moss AA. Difference between liver and spleen CT numbers in the normal adult: Its usefulness in predicting the presence of diffuse liver disease. Radiology 1980;137:727-9.
15. Raptopoulos V, Karellas A, Bernstein J, Reale FR, Constantinou C, Zawacki JK. Value of dual-energy CT in differentiating focal fatty infiltration of the liver from low-density masses. Am J Roentgenol 1991;157:721-5.
16. Kodama Y, Ng CS, Wu TT, Ayers GD, Curley SA, Abdalla EK, *et al*. Comparison of CT methods for determining the fat content of the liver. AJR Am J Roentgenol 2007;188:1307-12.
17. van Werven JR, Marsman HA, Nederveen AJ, Smits NJ, Ten Kate FJ, van Gulik TM, *et al*. Assessment of hepatic steatosis in patients undergoing liver resection: Comparison of US, CT, T1-weighted dual-echo MR imaging, and point-resolved 1H MR spectroscopy. Radiology 2010;256:159-68.
18. Dixon WT. Simple proton spectroscopic imaging. Radiology 1984;153:189-94.
19. Fishbein MH, Gardner KG, Potter CJ, Schmalbrock P, Smith MA. Introduction of fast MR imaging in the assessment of hepatic steatosis. Magn Reson Imaging 1997;15:287-93.
20. Ma X, Holalkere NS, Kambadakone RA, Mino-Kenudson M, Hahn PF, Sahani DV. Imaging-based quantification of hepatic fat: Methods and clinical applications. Radiographics 2009;29:1253-77.
21. Skoch A, Jiru F, Bunke J. Spectroscopic imaging: Basic principles. Eur J Radiol 2008;67:230-9.

Cite this article as: Singh D, Das CJ, Baruah MP. Imaging of non alcoholic fatty liver disease: A road less travelled. Indian J Endocr Metab 2013;17:990-5.

Source of Support: Nil, **Conflict of Interest:** None declared.